

# Arrayed waveguide grating based on Si nanowire with two center wavelengths

MAHMOOD SEIFOURI<sup>a,\*</sup>, SAEED OLYAEE<sup>b</sup>, MARYAM AHMADVAND<sup>a</sup>

<sup>a</sup>Faculty of Electrical Engineering, Shahid Rajaei Teacher Training University, Tehran, Iran

<sup>b</sup>Nano-photonics and Optoelectronic Research Laboratory (NORLab), Shahid Rajaei Teacher Training University, Tehran, Iran

In this paper, a 23-channel arrayed waveguide grating (AWG) demultiplexer with two center wavelengths at 1550 nm and 1310 nm based on silicon nanowire has been presented. If the center wavelength is 1550 nm, the proposed structure operates as an 8-channel demultiplexer with a channel spacing of 1.6 nm and an insertion loss of 1.1 dB. Otherwise, with the center wavelength of 1310 nm, our structure behaves as a 15-channel demultiplexer with a channel spacing of 0.67 nm and an insertion loss of 1.2 dB. When tapered waveguides are introduced at both ends of all waveguides, the input, the output and the arrayed waveguides, the insertion loss reduces significantly. Therefore, transmission coefficient becomes very desirable in our structure. Simulations are carried out using the beam propagation method. Due to the minimal difference between the insertion loss of the center wavelength and the adjacent wavelengths, the spectral response of the proposed structure is relatively flat for both center wavelengths. The crosstalk values for the center wavelengths of 1550 nm and 1310 nm are respectively, -46 dB and -38 dB.

(Received June 6, 2017; accepted August 9, 2018)

*Keywords:* Arrayed waveguide grating, Center wavelengths, Crosstalk, Insertion loss, Silicon nanowire

## 1. Introduction

In recent years, all-optical networks have attracted great interest. These networks are used in an optical line terminators (OLT) or electronic switches and wavelength division multiplexer/demultiplexer (WDM/DMUX) networks [1]. The WDM networks are a high performance network that can have different channels for different purposes and increase bandwidth using multichannel techniques. Due to the growth of the use of the Internet, including the information transformation, multimedia communications, e-commerce, demand for bandwidth has increased further. One of the ways to increase bandwidth and having more channels are to use the WDM system to improve the network [2]. The all optical networks WDM provides almost infinitely bandwidth with re-use of optical fiber wavelengths [3]. To increase data transmission capacity of optical signals in optical fibers, dense wavelength division multiplexing (DWDM) can be used [4].

The arrayed waveguide grating (AWG) was first proposed by Smit [5] and further developed by Takahashi et al. [6]. Dragone [7] introduced  $N \times N$  wavelength routers, which play an important role in multi-wavelength network applications [8]. The AWG multiplex is widely used as a key component in coarse wavelength division multiplexer (CWDM) and dense wavelength division multiplexer (DWDM) networks [9,10]. The AWG multiplex device combines high wavelength selection with compression design and reduction insertion loss [11]. Arrayed Waveguide Gratings (AWGs) are considered an attractive

DWDM solution because they represent a compact means of offering higher channel count technology, have good performance characteristics, and can be more cost-effective per channel than other methods [12]. The passive optical network (PON) includes an OLT used by the AWG [13].

The costs and the complexity of the network are reduced significantly using arrayed waveguide grating in the wavelength routing functions [14]. The performance characteristics of AWGs depend on the optical properties of the waveguide materials used. AWGs are divided into two main groups, as far as the materials used are concerned. One group, including rectangular waveguides made up of for example,  $\text{SiO}_2$ , Silica-on-Silicon (SoS) [15], InP [16,17], silica [18] or polymer [19,20], has a small difference between the refractive index of the core and the cladding. In this group, the refractive index difference between the core (waveguide) and the cladding is about 0.75%, fiber coupling loss is low and is about 0.1 dB and the propagation loss is also low. However, to have a low index contrast, a very large bending radius of the waveguides is needed, which leads to the increase in the dimensions of the device.

The other group, including waveguides made up of silicon nanowires [21], Silicon-On-Insulator (SOI) [22-24] and silicon [25], has a large difference between the refractive index of the core and the cladding. The refractive index difference in this group is about 58%. This is approximately one hundred times higher than that of typical SoS waveguides. The dimensions of the arrayed waveguides are reduced by increasing the difference

between the refractive index of the core and the cladding. Consequently, the dimensions of the arrayed waveguides can be reduced to sub-micron scale. Therefore, with a high refractive index difference, light guiding is possible in an arrayed waveguide with a very small bending radius and this leads to the smaller dimensions of the device [26]. Such compact devices can easily be implemented on-chip and have already found applications in WDM systems especially in metro networks [12] and also in applications such as optical Q-switch [27]. The problem with this structure is the coupling of light into the fiber, which leads to high coupling losses of about 10 dB [28]. Silicon is one of the elements that is widely found in nature; therefore, the majority of optical communication systems use silicon-based optical integrated circuits and systems. Using silicon in optical integrated circuits leads to reduced speed, increased noise, and reduced efficiency; we can use all-optical devices in order to overcome these problems [29].

In recent years, AWG based on silicon nanowire waveguides [30–37] has attracted much attention for its compact size owing to the large-index-difference property of the SOI waveguide, which allows for sharp bends. Moreover, its fabrication is compatible with CMOS technology, offering a promising solution for large-scale integration with other silicon-based devices in a high-density photonic chip [38].

Three wavelength bands with wavelengths around 850 nm, 1310 nm and 1550 nm are the considered in telecommunication and devices operating in WDM systems are such implemented having good performance

in desired wavelength [8,39]. Unlike conventional demultiplexer which has only one center wavelength, the proposed AWG demultiplexer operates at two center wavelengths, namely, 1550 nm and 1310 nm. In addition, due to using silicon nanowire waveguides, the structure is relatively compact as compared to [39]. In [39], the arrayed waveguides are chosen each with a width of 4  $\mu\text{m}$ . The proposed structure operates at the center wavelength of 1550 nm as an 8-channel AWG with a channel spacing of 1.6 nm. Otherwise, it behaves as a 15-channel AWG with a channel spacing of 0.67 nm, at the center wavelength 1310 nm.

This paper is formed as follows, in Section 2, focuses on AWG principle. Section 3 analysis and design of AWG is described. In Section 4, simulation results are investigated are presented. Finally, the Conclusions is provide in Section 5.

## 2. AWG principle

As shown in Fig. 1, the structure of an arrayed waveguide grating (AWG) demultiplexer consists of input and output waveguides, two free propagation regions (FPRs), and arrayed waveguides. The arrayed waveguides are paths to connect two FPRs. Firstly the light becomes divergent in the first FPR and then, the divergent beam is propagated in the arrayed waveguides with different path lengths being a function of the center wavelength and finally reach the second FPR [40].

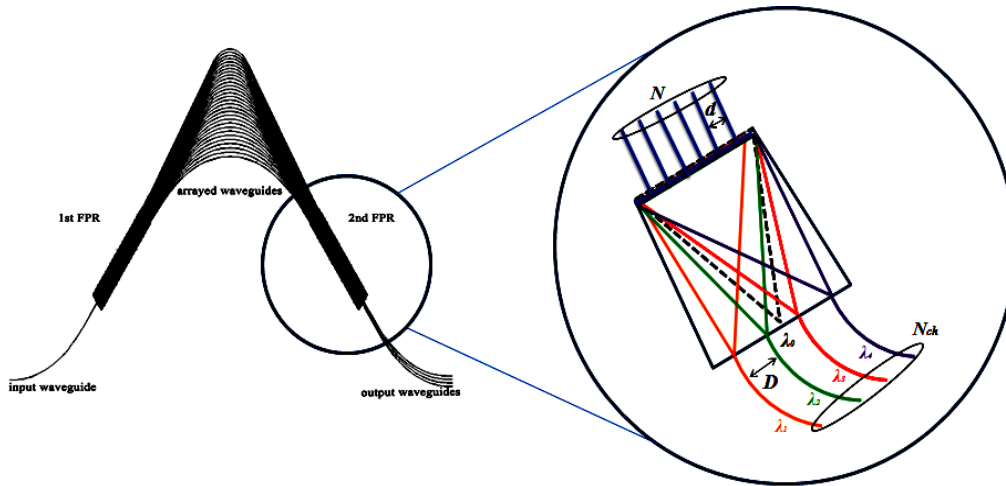


Fig. 1. The structure of conventional AWG demultiplexer

In the arrayed waveguides, there is a constant phase difference between two each adjacent waveguides and this phase difference depends on the wavelength. The optical path length difference,  $\Delta L$ , between two successive waveguides in the array is constant.  $\Delta L$  can be expressed as follows [41]:

$$\Delta L = \frac{m\lambda_0}{N_{eff}} \quad (1)$$

where  $m$  is the grating order,  $\lambda_0$  is the center wavelength of the grating and  $N_{eff}$  is the effective index of the arrayed waveguide.

### 3. Analysis and design of AWG

In the arrayed waveguide grating, the number of waveguides must be designed in such a way that the low insertion loss and flat spectral response can be achieved. In the proposed structure, the arrayed waveguide grating has been considered as having 8-channel with a channel spacing of 1.6 nm. This AWG is based on silicon nanowire with a waveguide refractive index of 3.7 and an effective refractive index of 2.8. The arrayed waveguides are chosen with a width of 500 nm and a height of 300 nm. The diameter of the nanowire is 500 nm. In the proposed structure, the multi-wavelength light after propagating through the first FPR and through the AWG structure is demultiplexed. The amounts of loss and the crosstalk depend on the number of waveguides in the array. So, one of the important criteria for having a device with good performance is the right choice of the number of the arrayed waveguides. Also, both ends of all waveguides, including the input, the output and the arrayed waveguides are tapered. In addition, the length and the width of the tapered sections are considered to be equal to 2  $\mu\text{m}$  [38] and 1  $\mu\text{m}$  [8,38], respectively. In the proposed structure, to determine the number of channels, Eq. (2) has been used [42].

$$N_{ch} = \frac{\lambda_0 R}{n_s d D} \quad (2)$$

Where  $n_s$  are the effective index of the slab region,  $R$  is the minimal length of the free propagation region, and the effective index of arrayed waveguide,  $d$  is the distance between the adjacent input arrayed waveguides, and  $D$  is the distance between the adjacent receiver waveguides.

To determine the number of the arrayed waveguides, Eq. (3 and 4) has been used [42].

$$N = 2\theta R/d + 1 \quad (3)$$

Therefore,

$$N = 2\theta \frac{N_{eff} \Delta\lambda D}{\lambda_0 d} N_{ch} + 1 \quad (4)$$

Where  $\theta$  and  $\Delta\lambda$  are the aperture angle and the channel spacing, respectively.

After determining the number of the arrayed waveguides, the device can be designed in such a way that in addition to operation at the center wavelength of 1550 nm, it can also be applicable at center wavelength of 1310 nm. Therefore, the proposed structure is very suitable for telecommunication applications. The schematic of AWG silicon nanowire is shown in fig. 2(a). According to Fig. 2(a), in the proposed structure, the arrayed waveguide grating (AWG) has been considered as having 8-channel at a wavelength of 1550 nm with a channel spacing of 1.6 nm. Using the relationships outlined in the paper, we construct a structure that works at a wavelength of 1310 nm in the form of a 15-channel demultiplexer with a channel spacing of 0.67 nm. This AWG is based on silicon nanowire with a waveguide refractive index of 3.7 and an effective refractive index of 2.8. The arrayed waveguides are chosen with a width of 500 nm and a height of 300 nm. The diameter of the nanowire is 500 nm. The maximum bending angle for nanowire waveguides equal to 90°. The AWG is formed by  $\pi$ -shape pattern. Fig. 2(b) shows the schematic of the output waveguides for (1b) AWG with  $\lambda_0 = 1550$  nm, (2b) AWG with  $\lambda_0 = 1310$  nm, and (3b) the proposed AWGs.

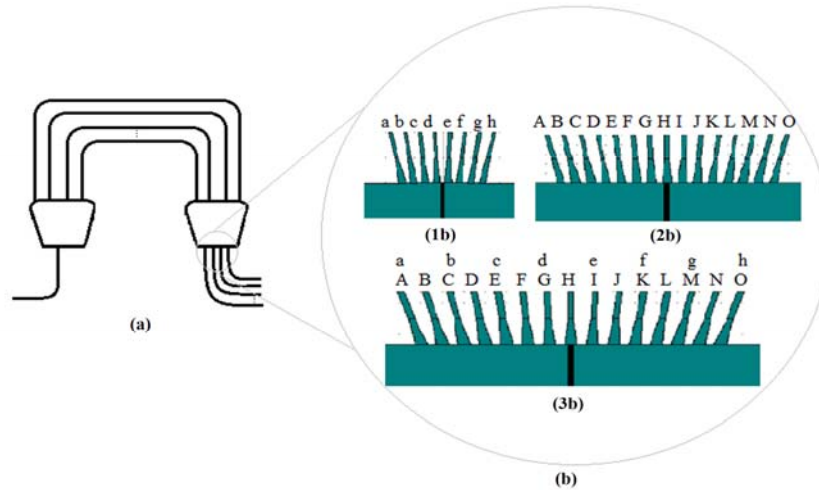


Fig. 2. Schematic of: (a) AWG Si nanowire, (b) the output waveguides for (1b) AWG with 8-channel, (2b) AWG with 15-channel, and (3b) the proposed AWGs

The following two equations for grating order  $m$  are the most important design equations of an AWG [8,39]:

$$m = \frac{\lambda_0 N_{eff}}{N_g N_{ch} \Delta\lambda} \quad (5)$$

$$N_g = N_{eff} - \lambda_0 \frac{\partial N_{eff}}{\partial \lambda}, \quad (6)$$

where  $N_g$  and  $\Delta\lambda$  are the group index and the channel spacing, respectively. We considered a silicon nanowire-based  $1 \times 8$  AWG with  $\lambda_0=1550$  nm and channel spacing of 1.6 nm. Choosing 62 arrayed waveguide with width of 500 nm, which is a typical size for such a silicon nanowire-based AWGs. If we design an AWG with above geometry, but operating in wavelength bands around 1310 nm, we can reach to an AWG with two central wavelengths with combination of two AWGs. Geometrical sameness can be shown by [8,39]

$$\frac{m\lambda_0}{N_{eff}} = \frac{m'\lambda'_0}{N'_{eff}} \quad (7)$$

$$\frac{N_s D d}{m \Delta \lambda} = \frac{N'_s D' d'}{m' \Delta \lambda'} \quad (8)$$

$$\Delta \lambda' = \left( \frac{D' d'}{D d} \right) \left( \frac{N'_s m \Delta \lambda}{N_s m'} \right) \quad (9)$$

$$N'_{ch} \Delta \lambda = \frac{\lambda'_0 N'_{eff}}{m' N'_g} \quad (10)$$

$N_g$  and  $N_s$  are respectively the group refractive index of arrayed waveguide and the effective refractive index of the two FPRs. The parameters with prime symbol are related to the AWG which is designed and work at the center wavelength of 1310 nm.

According to the Eqs. (5)-(10), the values of the parameters calculated for both the 8-channel and 15-channel AWGs are presented in the Table 1. Since the output waveguides should not overlap one another, therefore, the distance between the adjacent output waveguides of the 8-channel demultiplexer is twice that of the 15-channel demultiplexer ( $D=2D'$ ).

According to Eq. (1), we obtain the distance between the proposed Arrayed waveguide grating (AWG). Given the Eq. (2), we determine the number of AWG channels. The amounts of loss and the crosstalk depend on the number of waveguides in the array. So, one of the important criteria for having a device with good performance is the right choice of the number of the arrayed waveguides. Since loss and crosstalk are important in the structure, the number of arrayed waveguide obtained by Eq. (3) and (4) are obtained. The second point is to design the structure in such a way that it can work simultaneously on two wavelengths (1550 nm and 1310 nm). Using Eq. (5) to (10), the structure with two distinct central wavelengths are designed. The nanowire effect leads to decrease the bending radius and width of waveguides, Because the structure has compact. The governing equations do not change in structure, only design-related values have changed.

Table 1. Design parameters for the three types of discussed AWGs

	$\lambda_0$ (nm)	$\Delta\lambda$ (nm)	$N_{ch}$	$N_g$	$D$ ( $\mu\text{m}$ )	$d$ ( $\mu\text{m}$ )	$\Delta L$ ( $\mu\text{m}$ )	$m$
AWG1	1550	1.6	8	3.76	5.6	3.2	36.68	89
AWG2	1310	0.67	15	3.78	2.8	3.2	36.21	103
Proposed AWG	1550, 1310	1.6, 0.67	23	3.7	5.6, 2.8	3.2	36.4	89, 103

Notably, when the center wavelength is 1550 nm, our structure behaves as an 8-channel structure with a channel spacing of 1.6 nm. If the center wavelength is 1310 nm, our structure operates as a 15-channel structure with a channel spacing of 0.67 nm. The parameters of the first (AWG1 with  $\lambda_0 = 1550$  nm), second (AWG2 with  $\lambda_0 = 1310$  nm) and the new designed (Proposed AWG with  $\lambda_0 = 1550$  nm and 1310 nm) AWG demultiplexers are listed in Table 1.

The proposed structure is very suitable for lowering the insertion loss, making it flat and also for reducing the crosstalk. To the extent that we have investigated the literature, there is no report so far on such an arrayed waveguide grating based on silicon nanowire with two center wavelengths.

#### 4. Simulation results

The proposed 8-channel silicon nanowire AWG has been simulated with a center wavelength of 1550 nm, channel spacing of 1.6 nm, bending radius of 3  $\mu\text{m}$  and 62

arrayed waveguides by the beam propagation method (BPM) under TE polarization. The sensitivity of this structure to polarization is negligible. Thus, the output of the proposed structure doesn't depend on polarization. This AWG is based on silicon nanowire with a waveguide refractive index of 3.7 and an effective refractive index of 2.8. The length needed to make a phase difference is calculated to be 36.4  $\mu\text{m}$ . Both ends of all waveguides, including the input, the output and the arrayed waveguides are tapered. In addition, the length and the width of the tapered sections are considered to be equal to 2  $\mu\text{m}$  and 1  $\mu\text{m}$ , respectively. Simulations are performed in two stages: (1) level input light with wavelengths around 1550 nm are launched to the system, and the spectral response of AWG in this regime are then calculated; (2) light with wavelength band around 1310 nm is launched, and the transmission is extracted. A spectral response is obtained by output fields total of each waveguide. For simple analysis of spectral response, we consider crosstalk and insertion loss using, Eqs. (11) and (12) [43,44]:

$$crosstalk(dB) = 10\log_{10}\left(\frac{P_d}{P_u}\right) \quad (11)$$

$$insertionloss(dB) = 10\log_{10}\left(\frac{P_{in} - P_{out}}{P_{in}}\right) \quad (12)$$

In this case, the desired power  $P_d$  and the undesired power  $P_u$  at the output power. Also,  $P_{out}$  has the output power corresponding to the  $P_{in}$  input power. Fig. 3 shows the spectral response of AWG which operates at the center wavelength of 1550 nm with a channel spacing of 1.6 nm. The spectral response of each channel is shown with a specific color. For example, channel 5 is shown in pink color. Insertion loss occurs due to the diffraction at the interface of the planar waveguide and the arrayed waveguides. This value can be obtained using the spectral response diagram, as shown in Fig. 3. The insertion loss of this structure is calculated to be between 1.1 - 2.1 dB. According to the amount of insertion loss obtained, the data transmission is about 98.9%. According to Fig. 3, the crosstalk level for the 8-channel demultiplexer differs from -46 to -36 dB. Due to the slight difference between the insertion loss of the center wavelength and the adjacent wavelengths, it can be concluded that the spectral response of the device and the transmission are both flat.

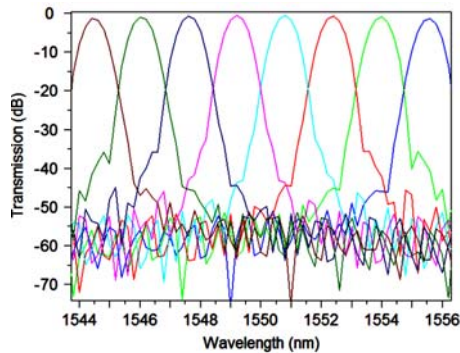


Fig. 3. Spectral response of AWG with  $\lambda_0 = 1550$  nm

Using the values shown in Table 1, the 15-channel AWG has also been simulated. Fig. 4 shows the spectral response of the proposed 15-channel AWG.

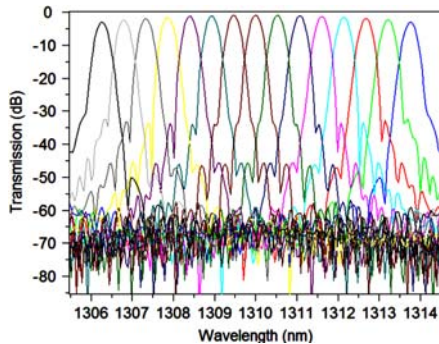
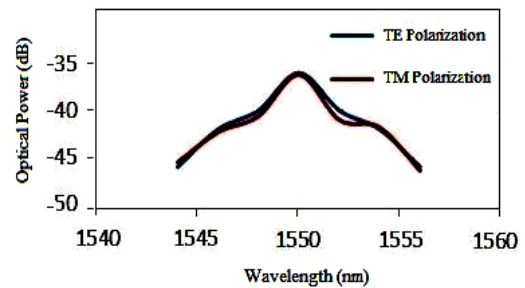


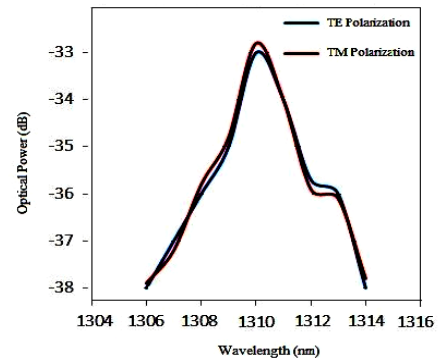
Fig. 4. Spectral response of AWG with  $\lambda_0 = 1310$  nm

From this figure, the insertion loss is calculated to be between 1.2 - 2.5 dB. Moreover, according to the same figure, the crosstalk level for the 15-channel demultiplexer differs from -38 to -32 dB. Table 2 shows the minimum and maximum values of the insertion loss and the crosstalk for both center wavelengths of 1310 nm and 1550 nm.

Fig. 5(a) and (b) shows the optical power in terms of wavelengths for the proposed demultiplexer in two modes TE and TM. According to these figures, the optical power in the wavelength range is the same for both TE and TM modes. For example, the optical power in two modes of TE and TM at 1550 nm is -36 dB and -36.1 dB, respectively. As a result, the structure has very low sensitivity to the polarization.



(a)



(b)

Fig. 5. Schematic of the optical power for variation wavelengths both TE and TM polarization for: (a)  $\lambda_0 = 1550$  nm, (b)  $\lambda_0 = 1310$  nm

The 3dB bandwidth ( $\Delta\lambda_{3dB}/\Delta\lambda$ ) of 8 and 15 channels AWG demultiplexer are 68.75% and 55.22%, respectively. Table 3 describes the comparison between the key parameters of the proposed structures with other reported structures. It can be seen that in comparison with other structures reported up to now, our proposed AWG has a better performance for both center wavelengths in terms of both insertion loss and crosstalk.

Table 2. Insertion loss and crosstalk for the two center wavelengths

	8-channel	15-channel
min insertion(dB)	1.1	1.2
max insertion(dB)	2.1	2.5
min crosstalk(dB)	-46	-38
max crosstalk(dB)	-36	-32

Table 3. Comparison between the key parameters of the proposed structure with other structures

Structure	[4]	[8]		[16]	[20]	[23]		[24]	[25]	[39]		Proposed structure	
Number of channels	4	4	7	4	16	4	8	16	8	16	27	8	15
Channel spacing (nm)	0.8	0.8	0.33	20 6.4	0.8	0.8	2	20	3.2	1.6	0.68	1.6	0.67
Center wavelength (nm)	1550	1550.12	1310.12	1310	1550	1550	1550	1451	1550	1550.12	1310.12	1550	1310
Substrate	Si Nano wire	Si	Si	InP	Polymer	SOI	SOI	SOI	Si	Silica	Silica	Si Nano wire	Si Nano wire
Insertion loss (dB)	3.5	4 6.5	7.8 11.2	5 7	2.19	2.45	1.32	3.74	-	1 5.9	1.3 6.06	1.1	1.2
Crosstalk (dB)	-20	-22 -26	-10 -14	-24 -25	-40	-17.12	-21.37	-31.26	-33 -35	-20 -38	-10 -24.7	-46	-38

## 5. Conclusions

The proposed structure of the arrayed waveguide grating based on silicon nanowire, has been designed and simulated with two center wavelengths. The simulations are performed using the beam propagation method. Spectral response shows that 8-channel AWG with a channel spacing of 1.6 nm works when the center wavelength is 1550 nm. Otherwise, 15-channel AWG with a channel spacing of 0.67 nm operates at the center wavelength of 1310 nm. Considering the tapered waveguides at both ends of all waveguides, including the input, the output and the arrayed waveguides, the insertion loss is significantly decreased. Due to the minimal difference between the insertion loss of the center wavelength and the adjacent wavelengths, the spectral response of the proposed structure is relatively very flat for both center wavelengths. The benefit of our proposed structure for telecommunication applications is that the value of data transmission in percentage has improved, when compared to other reported structures. The data transmission factor for our proposed structure is approximately 98.9%. The crosstalk for the 1550 nm and 1310 nm center wavelengths are respectively, -46 dB and -38 dB. The insertion loss for the 1550 nm and 1310 nm center wavelengths are respectively, 1.1 dB and 1.2 dB.

## References

- [1] Y. Ye, H. Woesner, I. Chlamtac, Journal of the Chinese Institute of Engineers **29**(7), 1149 (2006).
- [2] S. N. Lee, I. S. Hwang, Journal of the Chinese Institute of Engineers **32**(4), 457 (2009).
- [3] J. T. Tsai, C. H. Lien, Journal of the Chinese Institute of Engineers **26**(5), 585 (2003).
- [4] A. Rostami, H. Sattari, F. Janabi-Sharifi, IEEE International Symposium on Optomechatronic Technologies (ISOT), 1 (2010).
- [5] M. K. Smit, Electronics Letters **24**(7), 385 (1988).
- [6] H. Takahashi, S. Suzuki, K. Kato, I. Nishi, Electronics Letters **26**(2), 87 (1990).
- [7] C. Dragone, IEEE Photonics Technology Letters **3**(9), 812 (1991).
- [8] H. Sattari, A. Abbasi, Fiber and Integrated Optics **30**(6), 389 (2011).
- [9] J. Tippinit, W. Asawamethapant, IEEE on Electrical Engineering/Electronics, Computer, Telecommunications and Information Technology (ECTI-CON), 2015 12th International Conference on, 1 (2015).
- [10] D. Dai, S. He, Fiber and Integrated Optics **22**(3), 141 (2003).
- [11] B. B. C. G. D. Culemann, E. Voges, Fiber & Integrated Optics **17**(4), 279 (1998).
- [12] D. Seyringer, C. Burtscher, S. Partel, J. Edlinger, A. Maese-Novo, P. Muellner, R. Hainberger, J. Kraft, G. Koppitsch, G. Meinhardt, IEEE 18th International Conference on on Transparent Optical Networks (ICTON), 1 (2016).
- [13] H. W. Hung, Y. L. Lee, C. W. Sung, C. H. Hsu, S. L. Lee, Journal of the Chinese Institute of Engineers **40**(1), 93 (2017).
- [14] G. Maier, M. Martinelli, A. Pattavina, E. Salvadori,

- Journal of Lightwave Technology **18**(2), 125 (2000).
- [15] P. Dumon, R. Kappeler, D. Barros, I. McKenzie, D. Doyle, R. Baets, Optics & Photonics International Society for Optics and Photonics 58970D (2005).
- [16] M. Zirngibl, C. Dragone, C. H. Joyner, IEEE Photonics Technology Letters **4**(11), 1250 (1992).
- [17] P. Pan, J. An, Y. Wang, J. Zhang, L. Wang, Y. Qi, X. Hu, Optics & Laser Technology **75**, 177 (2015).
- [18] R. Adar, C. H. Henry, C. Dragone, R. C. Kistler, M. A. Milbrodt, Journal of Lightwave Technology **11**(2), 212993).
- [19] B. Yang, Y. Zhu, Y. Jiao, L. Yang, Z. Sheng, S. He, D. Dai, Journal of Lightwave Technology **29**(13), 2009 (2011).
- [20] Y. Xu, H. Lin, Optik-International Journal for Light and Electron Optics **125**(3), 920 (2014).
- [21] Z. Sheng, D. Dai, S. He, Journal of Lightwave Technology **25**(10), 3001 (2007).
- [22] L. Wang, W. Bogaerts, P. Dumon, S. K. Selvaraja, J. Teng, S. Pathak, X. Han, J. Wang, X. Jian, M. Zhao, R. Baets, Appl. Opt. **51**(9), 1251 (2012).
- [23] S. Pathak, D. Van Thourhout, W. Bogaerts, Opt. Lett. **38**(16), 2961 (2013).
- [24] N. Juhari, P. S. Menon, A. A. Ehsan, S. Shaari, A. Jalar, B. Y. Majlis, IEEE International Conference on Computer Communications and Control Technology (I4CT), 157 (2015).
- [25] T. Ye, Y. Fu, L. Qiao, T. Chu, Opt. Express **22**(26), 31899 (2014).
- [26] H. Woesner, M. Maier, A. Wolisz, In ONDM, 51 (2002).
- [27] H. Ahmad, K. Z. Hamdan, F. D. Muhammad, S. W. Harun, M. Z. Zulkifli, Appl. Phys. B **118**(2), 269 (2015).
- [28] D. Martens, A. Z. Subramanian, S. Pathak, M. Vanslembrouck, P. Bienstman, W. Bogaerts, R. Baets, IEEE Photon. Technol. Lett. **27**(2), 137 (2015).
- [29] G. Moloudian, R. Sabbaghi-Nadooshan, M. Hassangholizadeh-Kashtiban, Journal of the Chinese Institute of Engineers **39**(8), 971 (2016).
- [30] W. Bogaerts, S. K. Selvaraja, P. Dumon, J. Brockaert, K. De Vos, D. Van Thourhout, R. Baets, IEEE Journal of Selected Topics in Quantum Electronics **16**(1), 33 (2010).
- [31] K. Okamoto, K. Ishida, Opt. Lett. **38**(18), 3530 (2013).
- [32] K. L. Li, J. S. Zhang, J. M. An, J. G. Li, L. L. Wang, Y. Wang, X. J. Yin, X. W. Hu, Optoelectronics Letters **13**(3), 161 (2017).
- [33] Z. Lei, A. Junming, Z. Jiashun, S. Shijiao, W. Yuanda, H. Xiongwei, Journal of Semiconductors **32**(2), 024010 (2011).
- [34] S. Pathak, M. Vanslembrouck, P. Dumon, D. Van Thourhout, W. Bogaerts, Opt. Express **20**(26), B493 (2012).
- [35] T. Tsuchizawa, K. Yamada, H. Fukuda, T. Watanabe, J. I. Takahashi, M. Takahashi, H. Morita, IEEE Journal of Selected Topics in Quantum Electronics **11**(1), 232 (2005).
- [36] D. Dai, L. Liu, L. Wosinski, S. A. H. S. He, Electronics Letters **42**(7), 400 (2006).
- [37] P. Dumon, W. Bogaerts, V. Wiaux, J. Wouters, S. Beckx, J. Van Campenhout, R. Baets, IEEE Photonics Technology Letters **16**(5), 1328 (2004).
- [38] J. Wang, Z. Sheng, L. Li, A. Pang, A. Wu, W. Li, X. Wang, S. Zou, M. Qi, F. Gan, Opt. Express **22**(8), 9395 (2014).
- [39] H. Sattari, Optik-International Journal for Light and Electron Optics **123**(9), 775 (2012).
- [40] A. S. Vanani, R. Ghayour, Optical Engineering **50**(10), 105004 (2011).
- [41] S. Pathak, M. Vanslembrouck, P. Dumon, D. Van Thourhout, W. Bogaerts, Journal of Lightwave Technology **31**(1), 87 (2013).
- [42] S. Shaari, M. S. Kien, IEEE Proceedings International Conference on Semiconductor Electronics (ICSE) 235(2000).
- [43] M. Y. Azab, M. F. O. Hameed, S. M. El-Hefnawy, S. S. Obayya, IET Optoelectronics **10**(1), 21 (2016).
- [44] T. Gyselings, G. Morthier, R. Baets, Journal of Lightwave Technology **17**(8), 1273 (1999).

\*Corresponding author: mahmood.seifouri@sru.ac.ir